Volume 1 | Number 1 | Jan 2013 | Pages 1–100

Journal of
Materials Chemistry C

Materials for optical and electronic devices
www.rsc.org/materialsC

ROYAL SOCIETY
OF CHEMISTRY

ROYAL SOCIETY
OF CHEMISTRY

www.rsc.org/materialsC

Journal of Materials Chemistry C

PAPER

Synthesis and fluorescence properties of nanoisland-structured SiOx/CuxO composite

Xu Lu,[a] Yohei Ishida,[a] Thanh Mai Nguyen,[a] and Tetsu Yonezawa[a, *]

A nanoisland-structured SiO_x (x ≤ 2)/Cu_xO (x ≤ 2) composite was prepared from a Cu-deposited Si wafer by electrochemical anodization in a hydrofluoric acid (HF)-and-ferric nitrate ($Fe(NO_3)_3$) electrolyte. The surface of the nanoisland comprised Cu, Cu oxides, Si nanoparticles and Si oxides. The distribution of elemental Cu on the surface was uniform. Cracks and native Cu-oxides in the deposited Cu layer are the two main factors for the formation of the nanoisland-structured surface. Different from the single red photoluminescence (PL) band emitted from the electrochemical anodized bare Si wafer, a dual-visible PL band with comparable intensities at red and blue ranges was observed. The red PL quenching did not happen in this Cu-ions -doped nanostructured Si due to the different distribution areas of Cu^+ and the red PL centre.The red PL originates due to oxygen defects in the band gap of Si nanoparticles/Si oxides; the blue PL is the consequence of the band-to-band transitions between $3d^{10}$ and $3d^9 4s^1$ of Cu^+ ions and the intra d → d band transition of Cu^{2+} ions in the interstitial vacancies of Si oxides. Compared with the electrochemical anodized bare Si sample with a single PL band, the nanoisland-structured SiO_x/Cu_xO composite emitting a dual-PL-band is more promising for fabricating white light emitters.

1. Introduction

Nanostructured silicon (Si) and the related researches have become hot topics in recent times. As the size of the Si particles reduces to less than 5 nm, some native properties such as band gap, and thermal and optical properties become drastically different from those of larger-sized Si. Phenomena such as fluorescence, surface plasmon resonance and surface-enhanced Raman scattering are available for Si-related materials[1–4] that extend the application areas of Si, especially Si-based optoelectronics. In general, the most common preparation method of nanostructured Si is electrochemical anodization in HF-containing organic solutions.[1] In this method, the obtained samples always show a porous morphology with a single visible photoluminescence (PL) band in the red region.[5,6] Therefore, to be used as a multi-visible-band emitting material such as a white light source, nanostructured Si should be in a combination with other fluorescence materials.[7]

Metal and metal oxides combined with nanostructured Si is an efficient way to enhance the performances of nanostructured Si composites.[8, 9] Various efforts have been devoted to research the combination of noble metals or noble metal oxides with nanostructured Si.[10–12] In comparison with other noble metals, copper (Cu) is a commonly used metal with a lower electrical

resistivity, lower cost, higher diamagnetism and electro-migration resistivity. Therefore, fabricating Cu and Cu-oxides/nanostructured Si composites have attracted much attention. Photocatalytic H_2 evolution capacity can also be enhanced by a nanocrystalline Cu_2O /Si nanowire core–shell composite.[13] The contact of p-type Cu oxides and n-type Si formed a heterojunction structure for applying to a photodiode.[14] While investigating the optical properties of Cu/Cu oxides/porous Si composites, various Cu-coated aged porous Si showed intense blue emission, while the native red PL from porous Si was quenched.[15] M. Naddaf et al. found that the PL emission from porous Si (PSi) was modified by making a CuO/PSi composite.[11] An additional weak blue PL peak besides the common red emission was detected in their sample; however, the intensity of the blue emission is not comparable to that of the red emission. The existence of blue emission from the CuO/porous Si composite is promising for research on the full-range PL emission of Si/Cu composites. Therefore, there is a demand for obtaining more intensive blue emission for dual/multiple band PL emitted by Si/Cu based composites.

So far, although nano Cu/Cu^+ can show blue emission,[16] Cu/nanostructured Si composites usually show either a single blue PL[17] as the presence of Cu^+ or Cu^{2+} disrupts the native red PL from nanostructured Si, or a single red PL due to the relatively weak blue PL centres. It is necessary to design Cu-Cu oxide/Si composites with a suitable structure to obtain the dual/multiple-band PL emission with intensive intensity. One approach is making the distribution of the Cu^+/Cu^{2+} and the red PL centres associated with Si/non-stoichiometric Si oxide nanoparticles well separated to avoid the mutual disturbance between them. For fabrication of such structures, in this study, we synthesized a nanoisland-structured SiO_x/Cu_xO composite via a two-step process. In the first step, a thin

Cu film was deposited on a Si substrate by magnetron sputtering; and in the second step, the Cu deposited Si wafer was electrochemically corroded in an aqueous electrolyte solution of HF and $Fe(NO_3)_3$. The thus-prepared sample showed a nanoisland surface morphology instead of the traditional porous one. Simultaneously, a dual-visible PL band was observed at the red and blue regions with comparable intensities. Introducing Cu-related defects on the surface resulted in the blue PL emission and its enhancement. In contrast to previous results,[18] the red PL quenching in Cu-ions -doped nanostructured Si did not happen due to the different distribution areas of the Cu^+/Cu^{2+} and the red PL centres on the surface of the prepared sample. Compared to traditional nanostructured Si that emits a single fluorescence band, the dual-band PL with comparable intensities from our sample is more promising for making white-light-emitting device.

2. Experimental method

2.1 Preparation of nanoisland –structured SiO_x/Cu_xO composite

First, Cu thin film was deposited onto a Si wafer by using a magnetron sputtering method as follows. The phosphorus-doped, <111>-oriented Si wafer (Nilaco, Japan), with an electrical resistivity less than 0.02 Ω·cm, was washed with ethanol and acetone by ultrasonic oscillation for 5 min, and then it was rinsed again with purified water. The pressure of the sputtering vacuum chamber was less than 5.0×10^{-3} Pa and then Ar gas was purged into the chamber at 2 Pa. The distance between the sample and the sputtering target was maintained at 60 mm. The sputtering current and period were set to 30 mA and 3 min, respectively. The thickness of the deposited Cu layer is estimated at ~10 nm. Then, the obtained SiCu sample was anodized in an electrolyte consisting of $Fe(NO_3)_3$ (0.008 mol· dm^{-3}, Junsei, Japan), HF solution (46 %, Stella Chemifa, Japan), and purified water (volume ratio, HF solution: H_2O = 7: 5 (v/v)) with a current density of 100 mA·cm^{-2} for 1 h. The obtained sample was washed by purified water and dried in air at room temperature.

2.2 Characterizations

Surface structure was observed by a JEOL JSM-6510LA scanning electron microscope (SEM), and surface composition analysis was carried out by a JEOL JPS-9200 x-ray photoelectron spectroscopy (XPS) device equipped with a monochromatic Mg Kα source operating at 100 W under ultrahigh vacuum (~1.0×10^{-7} Pa) condition; the obtained spectra were calibrated by the C 1s peak. Photoluminescence spectra were captured using a Jasco FP-6600 spectrofluorometer. A JEOL JIB-4600F/HDK multibeam system was used to process the FIB sample to obtain a final thickness less than 100 nm and the thus-prepared FIB sample was transferred to a molybdenum-grid transmission electron microscope (TEM) stage. The lateral structure, the related electron diffraction patterns and the energy-dispersive spectroscopy (EDS) spectra of the prepared sample were obtained by JEM-2010 transmission electron microscope (TEM, 200 kV).

3. Results and discussion

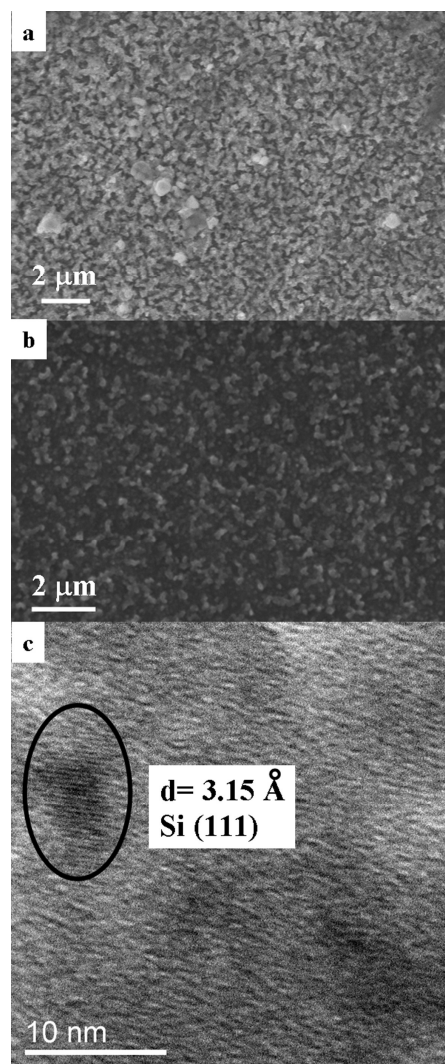### 3.1 Morphology, structure and composition of nanoisland-structured SiO_x/Cu_xO composite

Fig. 1. (a) Scanning electron microscope (SEM) image of the electrochemical anodized bare Si. (b) SEM image of the surface morphology of the anodized SiO_x/Cu_xO composite. (c) High-resolution transmission electron microscope (HR-TEM) image of the surface structure of the sample shown in (b), the measured interplanar distance of 3.15 Å corresponds to the Si (111) plane (3.13 Å).

Surface morphology of the as-prepared SiO_x/Cu_xO composite is shown in Fig. 1b. The isolated nanoisland is observed on the surface with a diameter of 200–500 nm. Compared with the surface of the anodized bare Si sample shown in Fig. 1a, the density of the nanoisland decreased and the distance among nanoislands increased. Moreover, the HR-TEM image (Fig. 1c) shows the Si

nanoparticles on the surface and the lattice fringes with distance of 3.15 Å, corresponding to distorted Si (111) (3.13 Å). These Si nanoparticles play an important role in changing the native properties due to the quantum confinement (QC).[1,9]
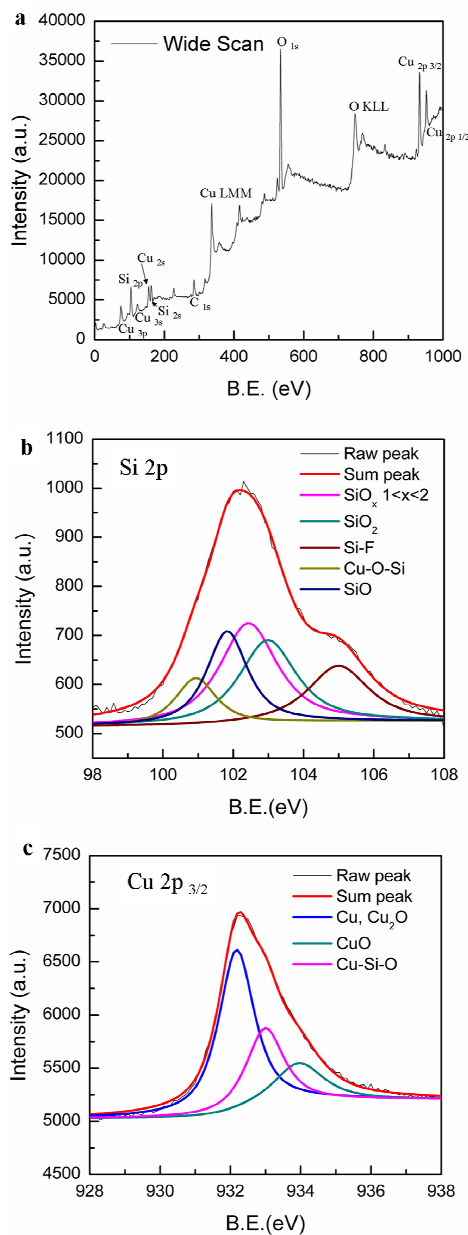

Fig. 2. **(a) XPS wide-scan spectrum of the freshly prepared nanoisland SiO$_x$/Cu$_x$O composite. (b) and (c) XPS narrow scan spectra of Si 2p area and Cu 2p$_{3/2}$ area of freshly prepared nanoisland SiO$_x$/Cu$_x$O composite, respectively.**

Surface composition analysis of the prepared sample was carried out by XPS as shown in Fig. 2. The wide-scan XPS spectrum shown in Fig. 2a indicated that the sample surface comprised Si, Cu, C and O (H cannot be detected by XPS, even though it may exist on the surface). Detailed narrow-scan XPS of Si 2p and Cu 2p$_{3/2}$ are shown in Figs. 2b and 2c. In the Si 2p spectrum, the main peak can be deconvoluted into five peaks at 100.8, 101.7, 102.5, 103.1 and 104.9 eV, which corresponded to Si–O–Cu, SiO, SiO$_x$ (1 < x < 2), SiO$_2$ and Si–F structures (in the order of increasing electro-negativity values of the elements bonded to Si from Cu to Si, O and F). F was not appeared in the wide-scan XPS spectrum, however, narrow-scan XPS can shows a weak F 1s peak (See Figure S1). Concurrently, narrow-scan XPS spectrum of Cu 2p$_{3/2}$ showed that the Si–O–Cu structure also presented in the spectrum of Cu 2p$_{3/2}$ area as well as the cuprous oxide and cupric oxide. The Cu ions are driven by electric potential and are moved into the protuberant nanoisland, these Cu ions may fill the interstitial vacancies (SiO, SiO$_x$) to form crystalline Cu and Cu-related defects (Si–O–Cu) that lead to blue PL. There was no characteristic peak of Si in the narrow-scan XPS spectra because the effective detection depth (less than 10 nm) of the XPS cannot reach the Si region, *i.e.*, after anodization, Si substrate was covered by Cu-oxides, Cu and Si-oxides, which will be discussed in Fig. 3.
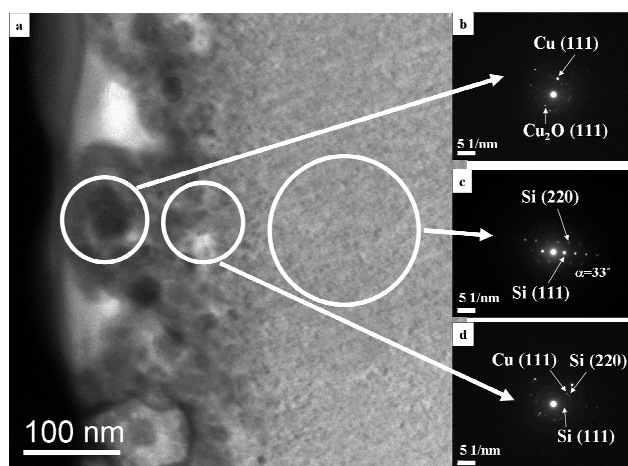

Fig. 3. **(a) TEM image of the lateral structure of the prepared SiO$_x$/Cu$_x$O composite (the sample was prepared by focused ion beam (FIB) treatment; the thickness was less than 100 nm after FIB treatment). (b)–(d) Electron diffraction patterns of the corresponding circle regions.**

Lateral morphology of the as-prepared nanoisland SiO$_x$/Cu$_x$O composited is shown in Fig. 3a. The height of the obtained nanoisland composite was ~150 nm. Simultaneously, different regions from the surface towards the Si substrate of the nanoisland composite were characterized by electron diffraction as shown in Figs. 3b–3d. Diffraction pattern of the protuberant area (80 nm from the substrate, Fig. 3b) showed only crystalline Cu$_2$O and Cu. The substrate is single-crystalline Si (Fig. 3c) and the sputtered Cu layer is only ~10 nm in thickness. The composition of the protuberant area was determined to be crystalline Cu$_2$O, Cu, amorphous Si oxides and amorphous CuO (as detected by XPS

spectra shown in Fig. 2c). At the junction region (Fig. 3d) of the protuberant area and the bulk Si substrate, the pattern of Si was detected, although it was very weak. This indicated that Si nanoparticles shown in Fig. 1c may have come from this junction region and this explained the absence of Si in the XPS spectra shown in Fig. 2b. This result further indicates that the Si nanoparticle area and Cu-oxides-concentrated area are separated. As the $Fe(NO_3)_3$ is an oxidant, compared to the sample prepared in the commonly used HF/ethanol electrolyte, the post-anodization oxidation degree of the outermost surface of our sample should be higher. In other words, the outermost surface is mainly composed of Si oxides, and Si nanoparticles are not concentrated on this region. However, from TEM image and diffraction results, Cu^+/Cu^{2+} is mainly distributed at the outermost surface, indicating that red PL disturbance from Cu^+/Cu^{2+} can be avoided, which is crucial for dual PL emission.

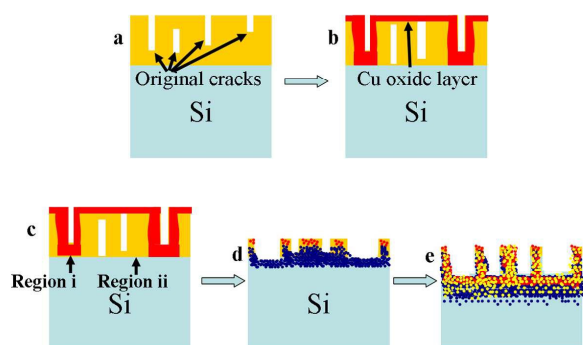### 3.2 *Formation mechanism of nanoisland-structured SiO_x/Cu_xO composite*

Fig. 4. **Schematic of the formation mechanism (Red: Cu oxides; Light blue: Si; Dark blue dots: Si oxides; Yellow: Cu). (a) Cu sputtered Si wafer; (b) Cu sputtered Si wafer in air; (c) anodization start; (d) intermediate corrosion; (e) final obtained sample.**

The schematic of the formation of the nanoisland-structured SiO_x/Cu_xO composite is shown in Fig. 4. Since the Cu cannot dissolve in HF, the key factors for the formation mechanism of nanoisland-structured SiO_x/Cu_xO composite are the native Cu oxides and the cracks in the Cu layer. As the Si surface is not an ideal surface, when a thin layer of Cu is deposited on the surface for a short period of time, it cannot form a continuous film due to surface tension (in our case, the thickness of the sputtered Cu layer was estimated at ~10 nm).[19] That means the thin layer of Cu on the surface exists in the isolated block fashion (see Figure S2). After Cu was sputtered on the Si surface, a thin original oxide layer will be formed automatically. This Cu oxide is soluble in acid solutions. At the beginning of the corrosion, the Cu oxides were first dissolved by HF, and then, there are two corrosion routes.

Region i: This is the region underneath the bottom of the deep cracks. After the original Cu oxides were dissolved, these areas may come in contact with the electrolyte. Hence, the Si in this area may

be corroded by the HF-containing electrolyte, as expressed in the below equations;

$$Cu_2O + 2HF \rightarrow 2CuF + H_2O \qquad (1)$$

$$Si + 4HF + 4h^+ \rightarrow SiF_4 + 4H^+ \qquad (2)$$
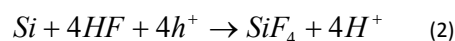
Region ii: This is the region underneath the Cu layer or the shallow, inner cracks. In these regions, after the original Cu oxides were dissolved, the Cu layer still remains thick enough, so that the corrosion speed became very slow. With help of the electric current, the Cu and the hydroxyl anion (OH^-) formed Cu_2O again, and then the corrosion is repeated as shown in equations (1), (2) and (3). This process is expressed as the following equations.

$$2Cu + 2OH^- \rightarrow Cu_2O + H_2O + 2e^- \quad (3)$$

$$Cu_2O + 2HF \rightarrow Cu_2F_2 + H_2O \qquad (4)$$
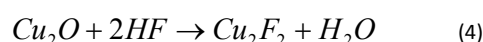
Finally, as the corrosion speeds of these two regions are different, the Cu-coated region became an island-shaped protuberance. In this case, the thickness of the Cu layer is a vital parameter for the formation of surface morphology as the cracks and native oxide layer conditions have a close relationship with the thickness of the deposited Cu layer. More surface morphologies of the anodized Cu deposited Si wafer samples with different Cu thickness are shown in Figure S3.

3.3 *Photoluminescence properties of nanoisland-structured SiO_x/Cu_xO composite*

The fluorescence spectra of the freshly prepared nanoisland-structured SiO_x/Cu_xO composite and the anodized bare Si are shown in Fig. 5a. Compared to the anodized bare Si, nanoisland SiO_x/Cu_xO composite showed two comparable PL bands at the red zone (peak centroid at 655 nm) and the blue zone (peak centroid at 469 nm). Compared to the reported Cu/nanostructured Si that has a single blue emission,[17,18] the quenching of the red PL usually associated with the Cu ions doping did not happen;[18] in comparison with Cu/nanostructured Si that has a single red emission,[11] the intensity of the blue emission was comparable with that of the red one. For the red PL from anodized bare Si, the mechanism involves the oxygen defects that are in the QC (arising from the Si nanoparticles).[20] In the case of nanoisland SiO_x/Cu_xO composite, the red PL still arose from the oxygen defects under QC effect. XPS spectrum (Figure 2b) and HR-TEM (Fig. 1c) image confirmed the presence of oxygen defects (SiO and Si_3O_4) and Si nanoparticles (nano size induces the QC effect[1]). One phenomenon that usually happens in Cu-ions-doped nanostructured Si is PL quenching because of the disruption of band-to-band transition due to the presence of Cu^+/Cu^{2+} impurities in the band gap.[18] However, in our case, it did not happen. From Figs. 3b and 3d, the Cu^+ and Cu^{2+} are mainly distributed in protuberance area while the red PL originated from the junction zone. The distribution of Cu oxides away from oxygen defect from Si oxides prevented quenching of the red PL. Concurrently, full-width at half-maximum (FWHM) of the red PL peak became wider due to the Cu ions diffused into the Si substrate

driven by electric potential and these ions were reduced to Cu (unlike Cu^+ and Cu^{2+}, pure Cu did not influence the native PL from nanostructured Si). So, the holes from the Cu ions may transport to the Si substrate to form more defects, broadening the PL peak in the red zone. Note that there was a small sub-band at 570 nm in the spectrum of nanoisland SiO_x/Cu_xO composite. This peak may be originated from the remaining Cu_2O as the band gap energy of Cu_2O is ~2.1 eV (590 nm).[21] In previous studies,[11,17] the blue peak was attributed to carbonyl compounds; however, in our case, the aqueous electrolyte solution of $HF/Fe(NO_3)_3$ did not contain any organic molecules. That means carbonyl compounds are not the reason for blue PL. In our case, the blue peak originated from the Cu-related defects which play the same role as a luminescent centre.[22–27]
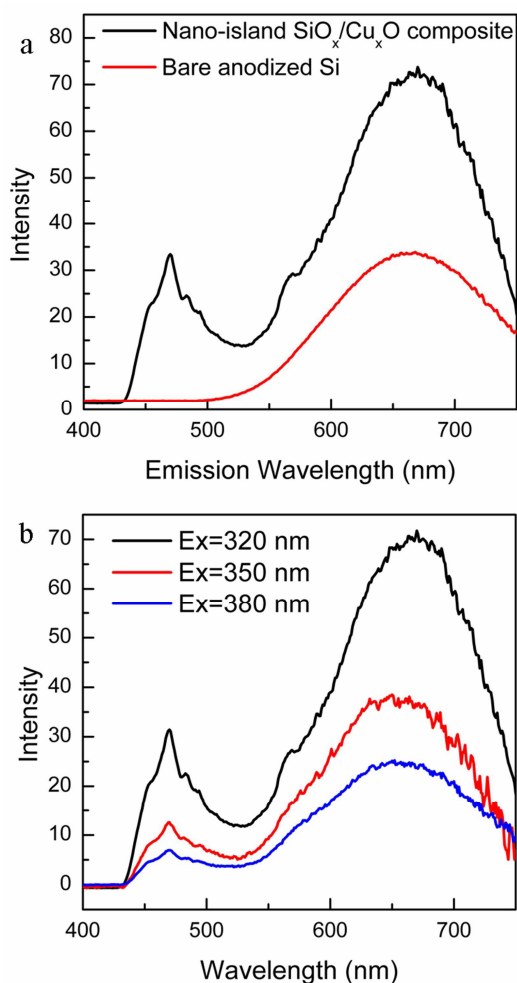

As the Cu has a high diffusivity[28] and Cu ion can be driven by electric potential, both Cu and Cu ions can diffuse into the protuberance layer. They will fill the interstitial vacancies and some of them may combine with the unstable SiO,[29] resulting in the formation of $Cu-SiO_x$ (Figs. 2b and 2c, Si–O–Cu).[15] All these defect states are PL centres. *e.g.*, Cu-related defects in the band gap of SiO_x that arose from $3d^{10} \leftrightarrow 3d^9 4s^1$ transitions of Cu^+ resulted in the blue emission.[15,23,24] The spikes in the blue peak are due to the intra d → d band transition of Cu^{2+}. In comparison with a previous report,[11] the relatively enhanced blue emission may be due to the uniform distribution of Cu on the surface. Previously reported samples showed a fibre columnar structure and the Cu elements were only concentrated at the top of the fibre columns, so, the blue PL centres were only present there. However, in our samples, Cu distribution was very uniform (See Table S1) on the surface, therefore, Cu defects can cover the entire surface area. The improved blue PL was the consequence of the increase in number of PL centres. From the spectra shown in Fig. 5b, under different excitation wavelengths, the two emission peaks appeared at identical positions and both these two peaks weakened in intensity as the excitation wavelength increased. This further confirmed that defects are the main reason for the visible fluorescence because of the constant value difference between the two defect levels.

4. Conclusions

In this study, a nanoisland-structured SiO_x/Cu_xO composite was synthesized by electrochemical anodization. The nanoisland surface consisted of Si oxides, crystalline Cu and Cu_2O, and amorphous CuO and Si nanoparticles. The formation mechanism of this nanoisland structure depended on the structure and oxidation of the sputtered Cu layer. Fluorescence spectrum of the freshly prepared nanoisland-structured SiO_x/Cu_xO composite showed two luminescence bands at red and blue zones and the intensities of these two bands are comparable. The obtained results came from the designed structure which allows well separated distribution between the red and blue PL centres in the SiO_x/Cu_xO composite. Compared to the single-PL-band sample, the dual-band one offers a promising approach for making white light emitters.

Acknowledgements

Notes and references

1   A. G. Cullis and L. T. Canham, *Nat.*, 1991, **353**, 335.

Fig. 5. (a) The fluorescence spectra of the freshly prepared nanoisland SiO_x/Cu_xO composite and anodized bare Si (the anodized bare Si was prepared by same method without Cu coating before electrochemical anodization. The emission spectra were collected at the excitation wavelength of 320 nm); (b) The fluorescence emission spectra of the freshly prepared nanoisland SiO_x/Cu_xO composite collected under different excitation wavelengths.

2   L. Gan, L, Sun, H. He and Z. Ye, *J. Mater. Chem. C*, 2014, **2**, 2668.
3   L. Tsakalakos, J. Balch, J. Fronheiser, and B. A. Korevaar, *Appl. Phys. Lett.*, 2007, **91**, 233117-1.
4   H. F. Wilson, L. McKenzie-Sell and A. S. Barnard, *J. Mater. Chem. C*, 2014, **2**, 9451.
5   T. Yanagishita, M. Imaizumi, K. Nishio and H. Masuda, *ECS Solid State Lett.*, 2013, **2**, P117.
6   H. Foll, M. Christophersen, J. Carstensen and G. Hasse, *Mater. Sci. Eng. R*, 2002, **39**, 141.
7   E. Kayahan, *J. Lumin.*, 2010, **130**, 1295.
8   Y. Fu, R. Yao and C. Cao, *J. Mater. Chem. C*, 2013, **1**, 6422.
9   L. Lin, X. Sun, R. Tao, J. Feng and Z. Zhang, *Nanotechnology*, 2011, **22**, 075203-1.
10   P. N. Vinod, *RSC Adv.*, 2013, **3**, 3618.
11   M. Naddaf, O. Mrad and A. Al-zier, *Appl. Phys. A*, 2014, **115**, 1345.
12   O. A. Yeshchenko, I. M. Dmitruk, A. A. Alexeenko, M. Y. Losytskyy, A. V. Kotko and A. O. Pinchuk, *Phys. Rev. B,* 2009, **79**, 235438-1.
13   Z. Xiong, M. Zheng, S. Liu, L. Ma and W. Shen, *Nanotechnology*, 2013, **24**, 265402-1.
14   R. A. Ismail, *J. Semicond. Tech. Sci.*, 2009 **9**, 51.
15   X. Lu, Y. Ishida and T. Yonezawa, *New J. Chem.*, 2015, DOI: 10.1039/C5NJ00909J.
16   M. Chiba, M. N. Thanh, Y. Hasegawa, Y. Obora, H. Kawasaki and T. Yonezawa, *J. Mater. Chem. C*, 2015, 3, 514.
17   K. Y. Suh, Y. S. Kim and H. H. Lee, *J. Appl. Phys.*, 2002, **91**, 10206.
18   D. Andsager, J. Hilliard, J. M. Hetrick, L. H. AbuHassan, M. Plisch and M. H. Nayfeh, *J. Appl. Phys.*, 1993, **74**, 4783.
19   D. K. Polyushkin, E. Hendry, E. K. Stone and W. L. Barnes, *Nano Lett.*, 2011, **11**, 4718.
20   T. Nakamura, T. Ogawa, N. Hosoya and S. Adachi, *J. Lumin.*, 2010, **130**, 682.
21   M. Izaki, T. Shinagawa, K. T. Mizuno, Y. Ida, M. Inaba and A. Tasaka, *J. Phys. D: Appl. Phys.*, 2007, **40**, 3326.
22   Y. Fujimoto and M. Nakatsuka, *J. Lumin.*,1997, **75**, 213.
23   G. Zhang, J. Long, X. Wang, W. Dai, Z. Li, L. Wu and X. Fu, *New J Chem.*, 2009, **33**, 2044.
24   M. Anpo, M. Matsuoka, Y. Shioya and H. Yamashita, *J. Phys. Chem.*, 1994, **98**, 5744.
25   P. Yang, M. K. Lü, C. F. Song, D. Xu and D. R. Yuan, *Phys. Stat. Sol.*, 2002, **231**, 106.
26   N. Negishi, M. Matsuoka, H. Yamashita and M. Anpo, *J. Phys. Chem.*, 1993, **97**, 5211.
27   H. Yamashita, M. Matsuoka, K. Tsuji, Y. Shioya and M. Anpo, *J. Phys. Chem.*, 1996, **100**, 397.
28   A. Mesli and T. Heiser, *Phys. Rev. B*, 1992, **45**, 11632.
29   L. Brewer and R. K. Edwards, *J. Phys. Chem.,* 1954, **58**, 351.

Graphical and textual abstract for the table of contents entry

Synthesis and fluorescence properties of nanoisland-structured SiO$_x$/Cu$_x$O composite

Xu Lu,[a] Yohei Ishida,[a] Thanh Mai Nguyen,[a] and Tetsu Yonezawa[a]

[a] *Division of Materials Science and Engineering, Faculty of Engineering, Hokkaido University, Kita 13, Nishi 8, Kita-ku, Sapporo, Hokkaido 060-8628, Japan*

(8 cm × 3.37 cm)
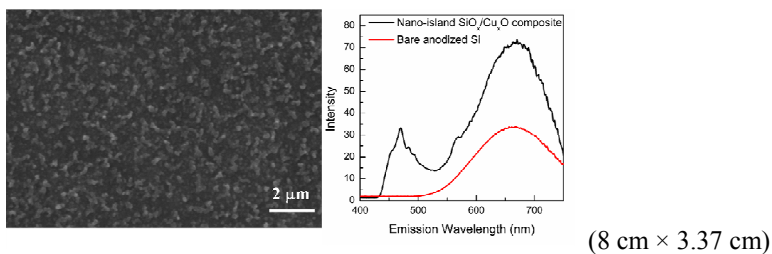
A dual-visible-band photoluminescence from SiO$_x$/Cu$_x$O composite was observed. The common red PL quenching phenomenon did not happen.